Resolving the Future of Astronomy with Long-Baseline Interferometry
ASP Conference Series, Vol. 487
Creech-Eakman, Guzik, and Stencel

Recent Observations of Betelgeuse and New Instrumentation at the ISI

S. Lockwood,[1] V. Ravi,[2] E. H. Wishnow,[1] W. Fitelson,[1] W. Mallard,[1]
D. Werthimer,[1] H. Mistry,[1] and C. H. Townes[1]

[1]*Space Sciences Laboratory, UC Berkeley, 7 Gauss Way, Berkeley, California 94720, USA; vravi@ssl.berkeley.edu*

[2]*School of Physics, University of Melbourne, Parkville, VIC 3010, Australia*

Abstract. The Infrared Spatial Interferometer (ISI) has been conducting mid-infrared observations of late-type stars for about 18 years. A long-term set of diameter measurements of Betelgeuse at 11.15 μm shows pronounced changes in the stellar size over time. These changes may arise from variations in the opacity of the environment immediately surrounding the star. New instrumentation is being developed to identify the composition and kinematics of the circumstellar environment of Betelgeuse, and of other late-type stars. A digital spectrometer-correlator is being built and tested that will enable visibility measurements on and off individual molecular spectral lines. Results from testing the spectrometer system are presented.

1. Introduction

The Berkeley Infrared Spatial Interferometer (ISI) is a three-telescope interferometer that operates in the mid-infrared spectral region (9–12 μm), and it is located at the Mt. Wilson Observatory. The telescopes have a Pfund optical design with 1.65 m diameter primary mirrors mounted in movable semi-trailers. The trailers can be placed at various locations at the ISI site, giving a range of baseline separations of 4 to 85 meters. The system is currently in a triangular configuration with baselines of ~36 m. The ISI is used to study giant, evolved stars and the gas and dust shells that surround them. Of particular interest are the sizes and shapes of these stars and their circumstellar environments, and the changes in these quantities with time.

1.1. Heterodyne Detection and Interferometry

The ISI uses $^{13}C^{16}O_2$ laser local oscillators in each telescope to down-convert starlight to radio-frequency (RF) baseband. Geometric delays are applied by switching lengths of coaxial cable, and signals from the three telescope pairs are combined to produce interference fringes. In this regard, the system is like a radio telescope array, but it operates near 27 THz.

The amplitudes and phases of the interference fringes provide high angular resolution information about sources. For telescopes with a baseline separation B, the angular resolution is proportional to $\lambda/2B$. The normalized fringe amplitude, or *visibility*, is

defined as

$$V = \frac{\mathrm{FP}}{\sqrt{P_1 P_2}},$$

where FP is the fringe power, and P_n is the total power detected by telescope n. When obtained at different baseline lengths, the visibility is a measure of the angular power spectrum of symmetric stellar features. The fringe phase determines the positions of features on stars. In the mid-infrared, however, atmospheric turbulence causes the phase to vary too fast to be calibrated. The ISI instead records *closure phase*:

$$\Phi_{\mathrm{CP}} = \phi_{12} + \phi_{23} + \phi_{31},$$

where ϕ_{mn} is the phase of the fringe between telescopes m and n, and all phases are measured simultaneously. Closure phase is not affected by turbulence, and it provides vital information about stellar asymmetries. For example, the closure phase is zero for sources that are centro-symmetric.

2. Observations of Betelgeuse

The red supergiant star Betelgeuse (α Ori) is among the best-studied stars. ISI diameter measurements over the last 18 years are shown in Figure 1. These measurements provide a new long-term observable for comparison to stellar theory and numerical models.

Observations in various optical and infrared bands show a patchy surface (e.g., Young et al. 2000; Haubois et al. 2009). Hotspots are predicted to arise from large convection cells on the surface (Schwarzschild 1975). ISI observations (Tatebe et al. 2007) revealed a possible hotspot on the southern edge of the star. The ISI was tuned to operate at 11.15 μm wavelength, between stellar molecular spectral lines, to probe the continuum emission. The results shown in Figure 1 are the uniform disk (UD) diameter fits to measured visibilities. All measurements were conducted using baselines of 32 m or longer. Measurements before 2006 were performed with a two-telescope system, and measurements since then were performed with three telescopes. The diameters plotted as diamonds were previously reported in Townes et al. (2009), where we noted a diminishing of the star's size over 16 years. These measurements were obtained by fitting a UD to the visibility data only, while not considering asymmetry. Since that time, we have continued to observe Betelgeuse and have seen an increase in size in 2009 and 2010. The points denoted by squares are fitted using both different data sets and a different technique. These diameters were determined by fitting models of uniform disks with offset point sources to account for asymmetries indicated by closure phase measurements. The model fitting of the 2006–2010 data is discussed in detail in Ravi et al. (2010, 2011). Over the three years 2006–2009, the two diameter determination methods coincide within the measurement errors. Pronounced variations of the diameter are not seen in the near-IR, and Ohnaka et al. (2011) has shown that the near-IR diameter of 43 mas changes only by ±2% over the period 1990–2010.

The absolute flux density of Betelgeuse has also been determined by comparing the total power within the ISI detection band to that of a calibrator, Aldebaran (α Taurus), with a flux density of 615 Jy at 11.15 μm (Monnier et al. 1998). The stellar flux density is then determined from the fractional flux of the UD component of the fitted model. Absorption and emission due to a thin dust shell at angular radii of about 1" are

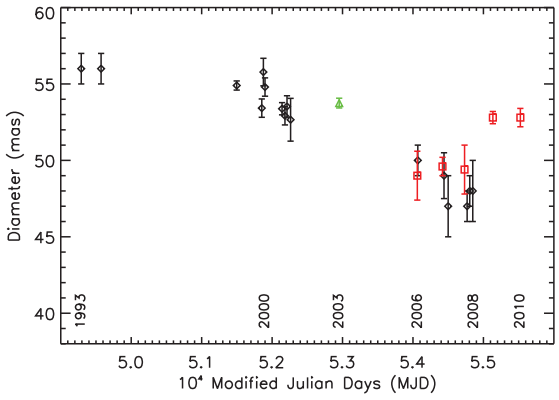

Figure 1. Diameter of Betelgeuse measured at 11.15 μm vs. time. Black diamonds, ISI (Townes et al. 2009); green triangle, 11.15 μm from Perrin et al. (2007) using the VLT interferometer; red squares, ISI recent results and re-analysis (Ravi et al. 2010, 2011).

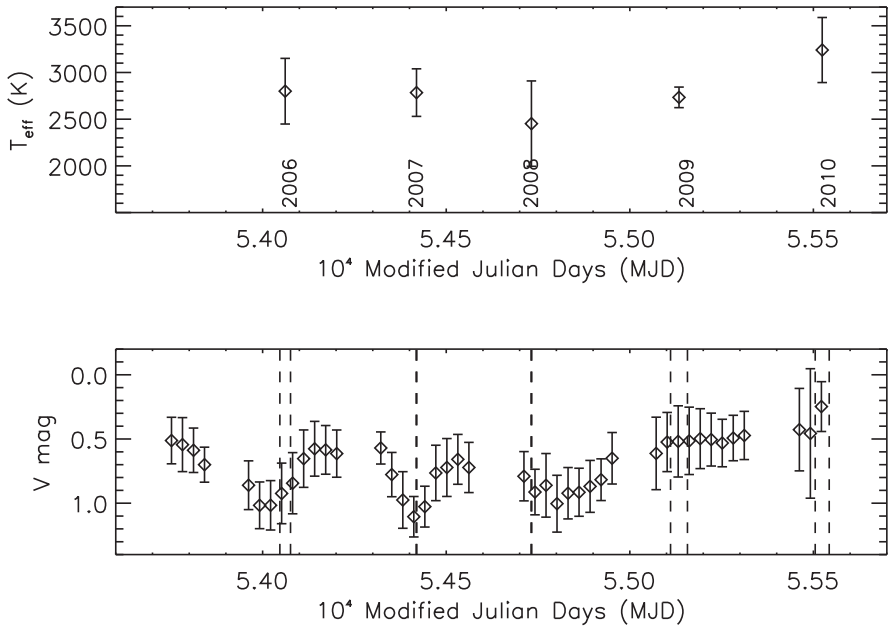

Figure 2. Top: effective temperatures of Betelgeuse at 11 μm for each observing epoch. The temperature is based on the stellar fraction of the total flux and uniform disk (UD) size. Bottom: corresponding V magnitude of Betelgeuse with our observations bounded by red lines. Each point represents a 30-day average of AAVSO data. From Weiner et al. (2003b).

not included in this estimate, but this shell is optically very thin (Danchi et al. 1994), and absorption by the interstellar medium is also not considered. The effective tem-

perature of the apparent stellar surface is then calculated from the stellar flux and the solid angle subtended by the UD. The effective temperatures for the period 2006–2010 are plotted in Figure 2. They are all considerably cooler than the nominal surface temperature of 3600 K measured in the near-IR (Perrin et al. 2007), indicating that mid-IR radiation is emitted from a larger and cooler region than near-IR radiation.

3. Interferometry with High Spectral Resolution

The 11.15 μm wavelength of the Betelgeuse observations corresponds to a spectral region that is free of strong spectral lines, so these measurements probe the stellar continuum. Previous mid-IR interferometry using low spectral resolution suggests that the continuum opacity could be due to Al_2O_3 dust (Verhoelst et al. 2006; Perrin et al. 2007). An additional continuum opacity mechanism is bremsstrahlung due to electron-hydrogen collisions (Tatebe & Townes 2006). In order to better understand the mid-IR opacity of stars, we are building a high-speed digital spectrometer-correlator for the ISI. These spectroscopic-interferometry measurements will determine the location and abundance of various molecular species surrounding AGB and supergiant stars.

At present, the ISI has a fairly high spectral resolution of 5000 (double sideband); the new spectrometer-correlator system will have a resolution of over 600,000 (the sidebands will be superimposed). Previous spectroscopic-interferometry using the two-telescope ISI configuration was performed using an analog filter bank to study the distribution of NH_3 and SiH_4 around IRC+10216 and VY Cma (Monnier et al. 2000). The new spectrometer-correlator uses high-speed FPGA (Field Programmable Gate Array) processors, and the work is being done in collaboration with the Center for Astronomical Signal Processing and Electronics Research (CASPER). Visibility and closure phase measurements will be obtained simultaneously on and off individual spectral lines.

Weiner et al. (2003a) conducted exploratory measurements of Mira in spectral regions with and without a water line using the full ISI bandwidth. Figure 3 shows that visibility measurements with a line in the band are fitted with a UD that is 20% larger than that fitted to the continuum region. The left panels of Figure 3 show TEXES high spectral resolution measurements of the two spectral regions. The dashed lines indicate the apparent Doppler shift of the ISI detection band due to the barycentric motion of the Earth. The "stick spectra" are predictions using the HITEMP/HITRAN database of H_2O line intensities at 1000 K (Rothman et al. 1998). The right panel shows the visibilities measured and UD fits in the two spectral bands.

Figure 4 shows the mid-IR spectrum of the Earth's atmosphere at frequencies below the ozone absorption band and "stick spectra" of OH and H_2O at 2500 and 1750 K, respectively. Initial studies will emphasize visibility measurements at frequencies of H_2O and OH lines, which are present in atmospheres of red supergiant and AGB stars. H_2O, OH lines, and continuum regions of interest are selected by predicting the molecular spectrum based on the stellar atmospheric temperature, the stellar recessional velocity, outflow velocity, and for gases that form at moderate distances from the star. A CO_2 laser line must then be selected so that a spectral line, or continuum region, falls within the ±2.8 GHz correlator bandwidth. Figure 4 shows two sets of laser lines for two isotopologues of CO_2 chosen to avoid absorption by telluric $^{16}O^{12}C^{16}O$.

The spectrometer-correlator system is currently being tested, and results from the first tests at Mt. Wilson are shown in Figure 5. Spectra of Venus around 10.884 μm were obtained simultaneously with two ISI telescopes on 03 February 2011. The sharp

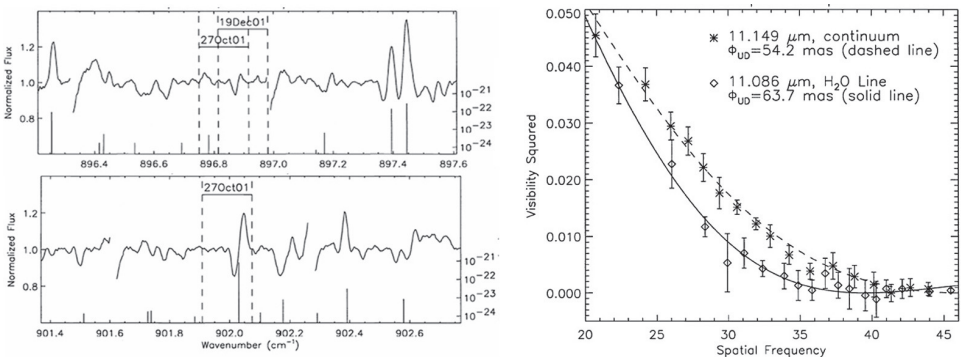

Figure 3. Left upper: continuum spectral region of o Ceti; dashed lines show ISI detection bands. Left lower: H_2O line region (Lacy et al. 2002; Rothman et al. 1998). Right: visibility squared of o Ceti, on-and-off H_2O line. The apparent size on-line is larger than the continuum size.

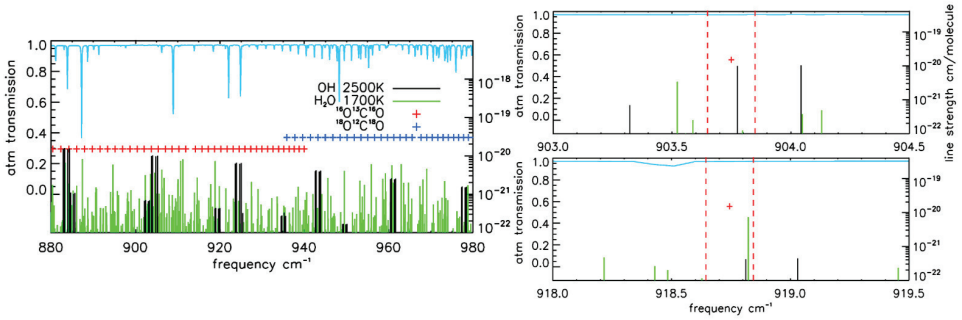

Figure 4. Left: atmospheric transmission vs. frequency (upper blue curve). Predicted intensities of OH and H_2O lines are shown as "stick spectra"; laser lines are indicated by red and blue + symbols. Right: two expanded regions of predicted stick spectra of α Ori for barycentric correction on 8 Nov. ISI detection bands are indicated by dashed red lines, which are centered on CO_2 laser lines. For this star, barycentric motion shifts the stellar lines with respect to the detection band by about $\pm 0.17\,\mathrm{cm}^{-1}$ over a year.

lines originate in the stratosphere of Venus, and despite the low abundance of $^{13}C^{16}O_2$, the R(6) line is comparable in strength to the P(46) line of $^{12}C^{16}O_2$. The P(46) line has rather low absorption due to the low population of the high molecular rotational energy state. A telluric line of $^{12}C^{16}O_2$ is centered at 768 MHz, but its effect is diminished due to the the lower frequency wing folding back into the detection band. This telluric line has a FWHM of 3 GHz due to pressure broadening, giving a breadth comparable to the spectrometer bandwidth. The spectrometer-correlator system complements the high spectral resolution capabilities of the Herschel Space Observatory, as although the ISI is not as sensitive, it has an angular resolution about 70X greater (Pilbratt et al. 2010).

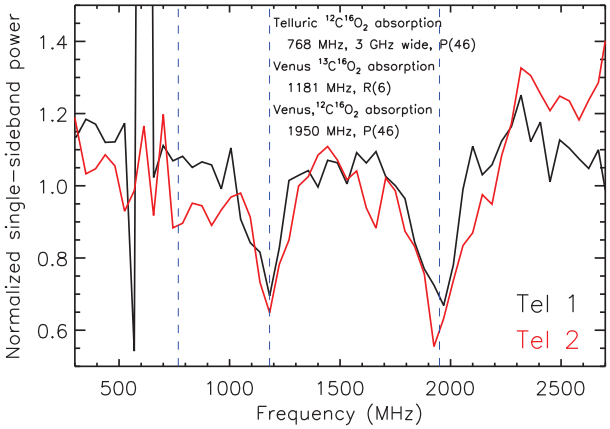

Figure 5. Mid-IR heterodyne spectra of Venus obtained on 03 February 2011 simultaneously with two telescopes (shown in black and red). The abscissa is the frequency offset from the $^{13}C^{16}O_2$ R(6) LO line at 918.744 cm^{-1} (10.884 μm). The same line in Venus' atmosphere appears at 1181 MHz due to the Doppler shift and the line at 1950 MHz is the $^{12}C^{16}O_2$ P(46) line. The broad curve is the telluric $^{12}C^{16}O_2$ P(46) line centered at 768 MHz; it is pressure broadened to a half-width of ~3 GHz. The 600 MHz region is contaminated by RFI. The data set involved chopping between the sky and a cold load at 140 Hz, and position switching on-and-off the source; the net time on-source was about 7 minutes.

Acknowledgments. We are grateful for support from Office of Naval Research, the National Science Foundation, and the Gordon and Betty Moore Foundation. This work also used observations from the AAVSO International Database.

References

Danchi, W. C., Bester, M., Degiacomi, C. G., Greenhill, L. J., & Townes, C. H. 1994, AJ, 107, 1469

Haubois, X., Perrin, G., Lacour, S., Verhoelst, T., Meimon, S., Mugnier, L., Thiébaut, E., Berger, J. P., Ridgway, S. T., Monnier, J. D., Millan-Gabet, R., & Traub, W. 2009, A&A, 508, 923. 0910.4167

Lacy, J. H., Richter, M. J., Greathouse, T. K., Jaffe, D. T., & Zhu, Q. 2002, PASP, 114, 153. arXiv:astro-ph/0110521

Monnier, J. D., Danchi, W. C., Hale, D. S., Tuthill, P. G., & Townes, C. H. 2000, ApJ, 543, 868. arXiv:astro-ph/0007418

Monnier, J. D., Geballe, T. R., & Danchi, W. C. 1998, ApJ, 502, 833. arXiv:astro-ph/9803027

Ohnaka, K., Weigelt, G., Millour, F., Hofmann, K.-H., Driebe, T., Schertl, D., Chelli, A., Massi, F., Petrov, R., & Stee, P. 2011, A&A, 529, A163+. 1104.0958

Perrin, G., Verhoelst, T., Ridgway, S. T., Cami, J., Nguyen, Q. N., Chesneau, O., Lopez, B., Leinert, C., & Richichi, A. 2007, A&A, 474, 599. 0709.0356

Pilbratt, G. L., et al. 2010, A&A, 518, L1+. 1005.5331

Ravi, V., Wishnow, E. H., Lockwood, S., & Townes, C. H. 2010, ArXiv e-prints. 1012.0377

Ravi, V., Wishnow, E. H., Townes, C. H., Lockwood, S., Mistry, H., & Tatebe, K. 2011, ArXiv e-prints. 1105.3273

Rothman, L. S., et al. 1998, JQSRT, 60, 665

Schwarzschild, M. 1975, ApJ, 195, 137

Tatebe, K., Chandler, A. A., Wishnow, E. H., Hale, D. D. S., & Townes, C. H. 2007, ApJ, 670, L21
Tatebe, K., & Townes, C. H. 2006, ApJ, 644, 1145
Townes, C. H., Wishnow, E. H., Hale, D. D. S., & Walp, B. 2009, ApJ, 697, L127
Verhoelst, T., Decin, L., van Malderen, R., Hony, S., Cami, J., Eriksson, K., Perrin, G., Deroo, P., Vandenbussche, B., & Waters, L. B. F. M. 2006, A&A, 447, 311. arXiv:astro-ph/0510486
Weiner, J., Hale, D. D. S., & Townes, C. H. 2003a, ApJ, 588, 1064
— 2003b, in SPIE Conference Series, edited by W. A. Traub, vol. 4838 of Presented at the SPIE Conference, 172
Young, J. S., et al. 2000, MNRAS, 315, 635